



# Investigation of Marine Sediments with a Sub-bottom Profilers System in West Coast of Camau, Vietnam

DUNG NGUYEN Quang<sup>1)</sup>, GIANG NGUYEN Van<sup>2)</sup>, THANH LE Ngoc<sup>3)</sup>

<sup>1)</sup> Institute of Geography and Resource in HCM city, 1 Mac Dinh Chi, distr. 1 HCM city, Vietnam <http://www.resourcesgeography.ac.vn>; ORCID 0009-0002-9232-5947

<sup>2)</sup> Binh Duong University, 504 Binh Duong Ave. Thu Dau Mot city, BinhDuong province, Vietnam, <https://www.bdu.edu.vn>; email: [nvgiang.hdkh@bdu.edu.vn](mailto:nvgiang.hdkh@bdu.edu.vn); ORCID 0000-0003-4477-430X

<sup>3)</sup> Institute of Geography and Resource in HCM city, 1 Mac Dinh Chi, distr. 1 HCM city, Vietnam <http://www.resourcesgeography.ac.vn>; ORCID 0009-0006-1685-915

\* Corresponding author: Giang Nguyen Van, [nvgiang.hdkh@bdu.edu.vn](mailto:nvgiang.hdkh@bdu.edu.vn)

<http://doi.org/10.29227/IM-2023-02-33>

Submission date: 14-08-2023 | Review date: 22-09-2023

## Abstract

The west coast of Camau (Southeast Vietnam) connects two semi-enclosed East Sea and Thailand Bays, allowing water exchange between them. Despite its importance to the oceanographic evolution of the region, it has still been poorly studied. Therefore, Sub-bottom profilers are used across shallow sea waters with some applications, such as sea-level studies, sedimentation process and geomorphology. In the whole survey area, 6 high-resolution shallow seismic measurements have been performed with a total length of 60.6 km, and all have recorded good reflected signals in the range 20–70 ms. In this section, physical characteristics and nature of petrology in the survey environment are quite uniformly shown. The topography of the seabed in the survey area tends to be gradually shallower from west to east, and is relatively flat. Particularly, on the cross section of the T1 line, it is visible that the first section of the line has a rather steep and deep terrain, which may be the slope of the continental shelf in the survey area. Wedge-shaped, oblique, corrugated and transverse structures all appear on the cross-sections. In the survey area, the shallow geological structure in the Holocene sediments is divided into 4 layers, and the structural boundary between the Holocene and Pleistocene sediments at the depth of 25–35 m is observed. In addition, geological faults are also detected on geological sections from seismic sections. For instance, at the section of T6 line, two faults were detected at the beginning of the line. The displacement amplitude of these faults ranges between 1.5–4 m. This new dataset will contribute to future comprehension of the geologic and oceanographic evolution.

**Keywords:** west coast of Camau, high-resolution shallow seismic, sub-bottom profiler, cross-section, Holocene-Pleistocene sediments

## Introduction

Coastal areas of Camau province have a special place in Vietnam's marine economic development strategy. By 254 km of coastline, enveloping Camau peninsula, adjacent to both the East and West Seas (Gulf of Thailand), the sea, coastal areas and island clusters in Camau province have a particularly important position in terms of national security and economic development of the country. In particular, the west coast of Camau province has an international biosphere reserve, including beach ecological areas, Camau mangrove forests, Camau flooded areas, Gulf of Thailand, protective forests coastal west Camau. Up to now, the coastal area along the west Camau sea area has not been studied in detail (Dung et al., 2013). Some of the meager research results have been published only on the surface of the geography, sea bottom shape, flow, waves and wind are the main (Lap et al., 2000). The study in detail of the geological structure of the coastal floor of Camau western province is an urgent requirement, especially for the planning of development of coastal construction works in Camau.

Among geophysical methods to survey the geological structure of the shallow waters, we have chosen a high-resolution seismic method that is the most appropriate one for the survey and determination of the shallow geological structure in this area. The main advantage of this method is compact

and lightweight device system, allowing detailed determination of geological structure sections with high accuracy (Alves et al., 2020; Amri, 2019; Aquino da Silva et al., 2016). However, because of single-channel registration, this method has limitations in anti-interference ability, especially in areas with complex geological structures (Lurton, 2002). Therefore, research to improve the effectiveness of their application is very necessary. This method is often used to study the shallow geological structure in the sea with a depth of several hundred meters (Grelowska et al., 2010; Saleh and Rabah, 2016). The research object of shallow geology and geophysics are mainly geological formations located in the upper part of the geological profiles, interesting for mineral prospecting and engineering geology (Kadima et al., 2011; Kozaczka et al., 2013). High-resolution shallow seismic equipment systems continuously emit and record reflected waves in the high frequency range of a few hundred to several thousand Hz, achieving horizontal resolutions of 3-5 m and vertical resolutions of 0.5-1m (Amri, 2019; Angulo et al., 2006; Aquino da Silva et al., 2016; Grelowska, 2010; Saleh, 2016; Wang et al., 2019). Because, the main objective of the study of the shallow sea area west of Camau was to determine the shallow geological structure for this coastal area limited to the Holocene sedimentary layer, and the Holocene-Pleistocene boundary, we utilised the system of Sub-bottom profilers. In recent decades,

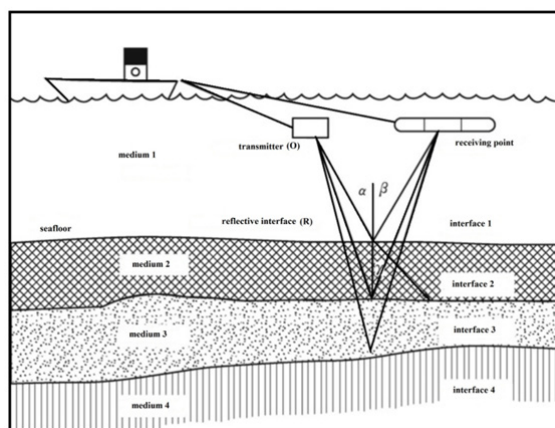


Fig. 1. Geometric kinematic model of acoustic signal for sub-bottom profiler detection (Modified of Ding et al., 2021)

Sub-bottom profiler has been widely used in underwater terrain measuring, hidden structure exploration, buried objects searching (Alves et al., 2020; LeBlanc, 1992; Ding et al., 2021). Beside the structure information in the data collected by profiler, the property of bottom sediment in shallow water also can be found out by inversion process. Therefore, our research area is limited to the west coast of Camau province with geographical coordinates as follows:  $8^{\circ} 38' 42.61'' - 9^{\circ} 31' 38.27''$  N and  $104^{\circ} 29' 52.72'' - 104^{\circ} 50' 3.14''$  E.

## Methodology and equipment

### High resolution shallow seismic method

#### Seismic waves

An underwater source of sound waves generates elastic waves that propagate with velocities depending on the elastic properties of the medium. Liquids do not react to shear waves (S-waves), so they cannot propagate in a liquid medium. Therefore, in marine surveys, it is only necessary to pay attention to the compression wave component (P-wave). Continuously reflected seismic signal is highly effective in the aquatic environment, because water is very effective in transmitting acoustic energy from the source to the layers of material below the seabed. Also, signal is of lower noise level, because is not affected by S wave part. The average speed of sound waves in seawater ranges 1.46 - 1.56 km/s depending on ambient temperature, salinity and pressure (depth). In the interpretation of seismic lines, the average value of wave propagation speed in the water layer is usually assumed to be equal to 1.5 km/s (Aquino da Silva et al., 2016; LeBlanc et al., 1992; Grelowska and Kozaczka, 2014).

The signal emitted from an acoustic source covers a range of different frequencies. To simplify the application of the discussed method, one often uses the concept of dominant frequency, which is the most common frequency or contains the maximum energy. The frequency of an acoustic signal ( $f$ ) is related to the wavelength ( $\lambda$ ) and the velocity ( $v$ ) of the acoustic wave according to the formula (Lurton, 2002):

$$\lambda = v/f \quad (1)$$

The dominant frequency of the sound wave source depends on the different types of equipment, ranging from 3.5 kHz to about a few hundred kHz. From formula (1), it can be seen that with the same wave propagation speed in the material medium, the higher the frequency of the emitted signal is,

the smaller is the wavelength, which means the higher resolution of the received signal.

When sound waves propagate in the wave propagation medium, energy attenuation will occur. There are three main mechanisms of this attenuation: (1) geometric attenuation, (2) energy absorption and frequency attenuation and (3) reflection and reverberation (Lurton, 2002). There are two types of repeaters, short repeaters and long repeaters. Short repeats arrive earlier than the main reflected wave and significantly reduce the original pulse or signal length, while long repeats represent a later arrival time (Kadima, 2011).

The phenomenon known as empty acoustic zones shows up on some shallow seismic tapes, especially in the coastal bays, where the reflections disappear suddenly beneath an almost horizontal layer in the bass column sediment. Because some types of sediments exhibit properties of absorbing or perturbing acoustic energy thereby both limiting energy penetration to deeper layers and impeding signals reflected upward from those strata (Grelowska and Kozaczka, 2010a).

### Sub-bottom profiler system equipment

The principle of sub-bottom profiler detection is similar to that of multi-channel reflection seismic exploration. First, a longitudinal acoustic wave is excited artificially, which during propagation can generate a reflection echo at the lithological interface of a formation. The reflected signal is received and stored by an acoustic transducer or a single receiving cable, and then the structure and shape of the submarine formation can be displayed in real time (3200-xs sub-bottom system user hardware manual, 2005). As shown in Figure 1, acoustic signals excited from transmitter O propagate in seawater and submarine sedimentary strata. As different lithological strata are encountered, in accordance with the principles of the geometry of seismic reflection, the incident wave generates  $\alpha$ , reflection wave at angle  $\beta$ , that is equal to incident angle  $\alpha$  at the interface. The transmission angle  $\gamma$ , is determined by the sound wave propagation velocity of the upper and lower layers at the interface. If the sound wave propagation velocity of medium 2 below the seafloor interface is greater than that of medium 1 above the interface, transmission angle  $\gamma$  is greater than incident angle  $\alpha$ , and vice versa. This case is only true when the distance between the receiver and the transmitter is large enough. In the case of only one channel as shown in Figure 1, it should be noted, because it may not be appropriate.

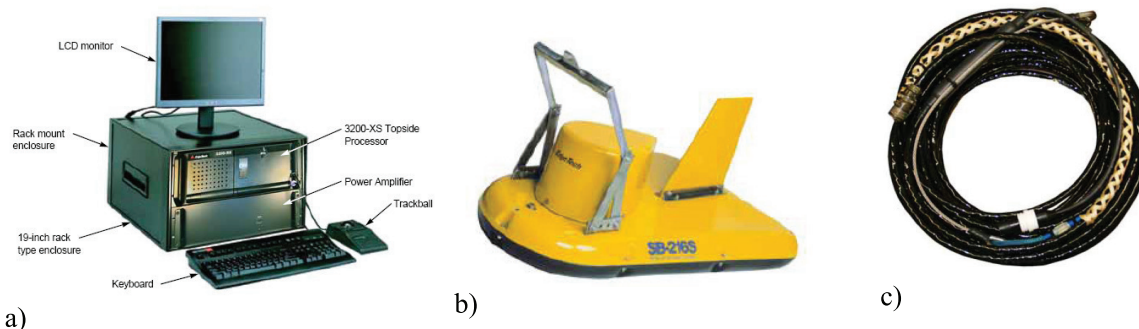


Fig. 2. Components of the Sub-bottom profiler measuring instrument system: a) 3200-XS Processing System, b) Towing device SB-216S, c) Kevlar Reinforced Tow Cable

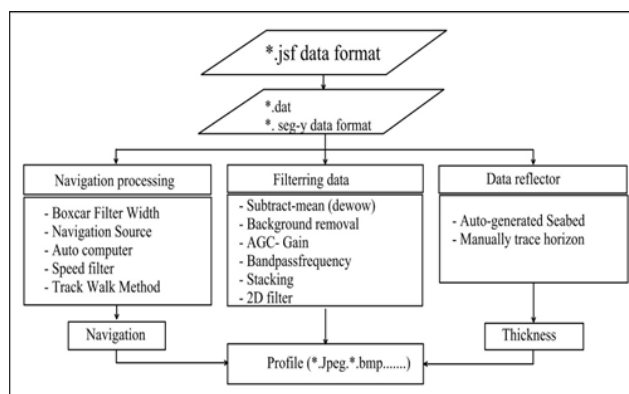


Fig. 3. Flow-chart of Sub-bottom profiler data processing

As the transmitted wave continues to propagate downward, new reflected and transmitted waves continue to be generated at subsequent acoustic impedance interfaces until the energy of the transmitted wave is too small to generate a reflected echo of effective energy. To form a strong reflective echo at an interface, there must be an obvious difference in the acoustic impedance condition at that interface.

The reflection coefficient,  $R$  can be expressed as follows (LeBlanc L.R. et al.,1992):

$$R = \frac{Z_2 - Z_1}{Z_2 + Z_1} = \frac{q_2 v_2 - q_1 v_1}{q_2 v_2 + q_1 v_1} \neq 0 \quad (2)$$

where  $q$  and  $v$  are the density of the sedimentary strata and the propagation velocity of sound waves within the strata, respectively, and their product is called wave impedance. Subscripts 1 and 2 denote the strata above and below the interface, respectively (Figure 1). According to the above equation, the condition that means the reflection interface can form a reflection echo is that  $q_2 v_2$  is not equal to  $q_1 v_1$ ; the greater is the difference between  $q_2 v_2$  and  $q_1 v_1$ , the stronger is the reflection echo energy. The greater is the amplitude of the reflection signal received by the transducer, the greater is the "gray value" of the acoustic reflection in-phase axis displayed by the recording section and the clearer the reflection strata interface. Therefore, a reflection interface is also called a wave impedance interface, which is consistent with the lithological interface of the actual strata and it represents different lithological horizons.

The Sub-bottom profiler is a high resolution broadband frequency modulation system that uses proprietary EdgeTech technology to generate cross-sectional images of the sub-bottom profiler. seabed and collects incident reflection data in digital form over multiple frequency ranges. This device

transmits a linearly scanned FM (frequency modulation) tone pulse over a full spectrum frequency range. Reflections in the measuring system are represented as gray streaks or other colors on a computer screen, which can be printed on a printer. Data is stored in real time in a large capacity hard drive. The Sub-bottom profiler system uses sound sources and receivers integrated in a tow vehicle to transmit and receive pulsed FM signals. The transmitters are wideband transducers and the receivers are hydrophone arrays of lead titanate/zirconate (PZT) crystals. The transducers are located in the inner part of the traction equipment and the receiver arrays. They are designed to operate out of ships, traveling at speeds of up to 7 miles/hour. The Sub-bottom profiler measuring instrument system is composed of 3 main components: (1) the processor which is located on the deck (3200 - XS), (2) the tow vehicle SB-216S and (3) kevlar fiber reinforced 75 m extension cable (Figures 2a, 2b, 2c), (3200-xs sub-bottom system user hardware manual, 2005).

The 3200-XS Sub-bottom profiler from the U.S. EdgeTech Corporation is adopted, which consists of towing fish, towing line and deck unit (Figure 2). The towing fish is of the type SB-216S and comprised of 1 transmitting transducer and 2 receiving transducers. The transmitted signal has a beam angle of  $24^\circ$  (-3dB). Sound boarding is used to separate the transducers in order to prevent the downward sound wave from interfering the received signal and to minimize surface reflection. The transducer transmits frequency modulated signal to the deep water right beneath it. The transmitted signal is able to penetrate into the stratum layers and will be reflected when the wave impedance changes. The reflected signal is received by the receiving transducer and sent to the deck unit through the towing line. A Topcon GPS system was connected with

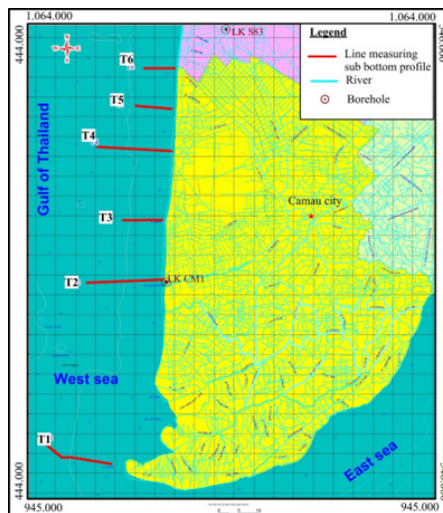


Fig. 4. The location of sub-bottom profiler measurement lines

the host machine of the deck unit. The GPS coordinate corresponding to each measuring point is extracted using the collection software. Flow-chart of data processing sub-bottom profiler was shown at Figure 3.

Sediment layers external shape and internal texture of sub-bottom profiler cross section records conducted using seismic facies analysis. This analysis was made to determine environmental depositing of seismic reflection characteristics, as well as continuity of amplitude, velocity, frequency and phase.

#### Geological characteristics of the study area

The study area is located on the west coast of Camau province, at the intersection of the East Sea and the Gulf of Thailand. The province of Camau is the low-lying area, with a typical height of 0.5-1 m above sea level. In Camau province the Cenozoic deposits are 300 m thick on average. The subsidence of the Mekong Delta basin in the Neogene was caused by the uplift of the Himalaya orogenesis, which was accompanied by high erosion rates in the mountains which provided large amounts of material, that formed the Mekong Delta sediments. Repeated cycles of marine transgression and regression during the Neogene and Pleistocene lead to a sequence of marine and terrestrial/alluvial facies. Glacial and events in the Pleistocene caused particularly strong regression and erosion (Stattegger et al., 2013). The stratigraphy, lithology, and facies of the unconsolidated sediments, are briefly described from the oldest to the youngest in the following sections on the base mainly on information from some boreholes with typical lithology and micro-paleontological evidence (Dung et al., 2013; Moley., 2002; Wagner et al., 2012).

#### Miocene (N1)

##### Upper Miocene, Phunghiep formation (N13ph)

The Phunghiep formation is the deepest unconsolidated sediment. Its thickness varies in the range 60-100 m. The bottom of these deep deposits, which corresponds to the top of the basement of the basin, dips gradually from the northwest to the southeast. The formation is unconformably covered by sediments of the Cấn Thơ formation (N21ct). The Late Miocene age (N13) formation consists of two facies: alluvial-marine deposits are overlain by marine deposits. There are the alluvial-marine deposits (amN13ph) and the marine deposits (mN13ph).

#### Pliocene (N2)

##### Lower Pliocene, Cantho formation (N21ct)

This formation is between 24-89 m thick in Camau province. It is unconformably covered by the younger Namcan formation. This sedimentary formation consists of 2-3 sedimentary cycles, each starting with coarse-grained sediments (sand, sandy silt) at the bottom and fining upward (silt, clay, clayey silt, silty clay, and silty sand). Based on the characteristics of the sediments and micro-paleontology, Cantho formation was formed in a delta landscape with bays, estuaries, and shallow sea. This formation is divided into two facies again, alluvial-marine deposits are covered by marine deposits.

##### Middle Pliocene, Namcan formation (N2nc)

These are the youngest Neogene sediments; there are no Upper Pliocene deposits. The thickness of the whole Namcan formation (N22nc) varies in the range 55-96 m, the average thickness is 79 m. It dips from the northwest to the southeast, and covers the sediments of the Cantho formation (N21ct) unconformably. There are two facies of this formation: alluvial-marine (amN22nc) overlain by marine deposits (mN22nc). These are fine-grained sediments (clay, silt, clayey silt) distributed throughout the region.

#### Pleistocene (Q1)

##### Lower Pleistocene, Camau formation (Q1cm)

Thickness changes in the range 36-87 m. The bottom of the Camau formation (Q11cm) dips gradually from northwest to southeast, and unconformably overlays the sediments of Namcan formation (N22nc). The Camau formation was formed in shallow marine environments of coastal mangroves and estuaries. This formation is divided into two facies: alluvial-marine deposits (amQ11cm); in Camau province area, the top of the amQ11cm deposits is located at depths between 84-154 m. Thickness varies in the range 19-77 m. Sediment composition includes mainly fine to medium sand; coarse and silty fine-grained sand; grey-brown silty sand containing a little gravel. The sediment is interbedded with silt layers. Marine deposits (mQ11cm): in the study area, are the top layer of the Camau formation and consists of fine-grained sediments. They are observed throughout the region and their thickness varies from a few meters to 35m.



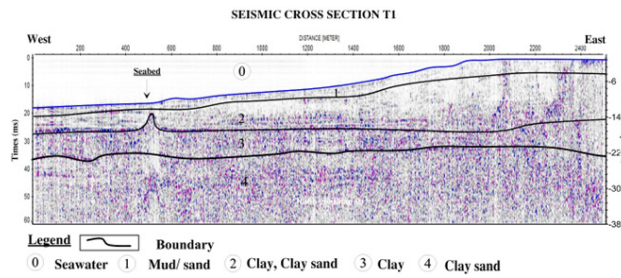


Fig. 5. The structural cross-section for seismic measurement line T1

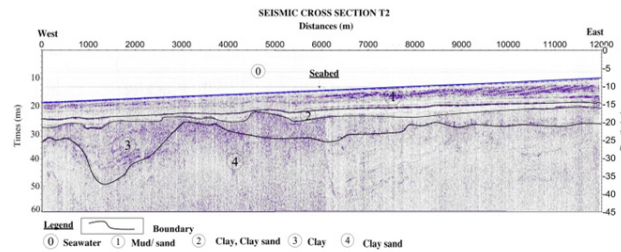


Fig. 6. The structural cross-section for seismic measurement line T2

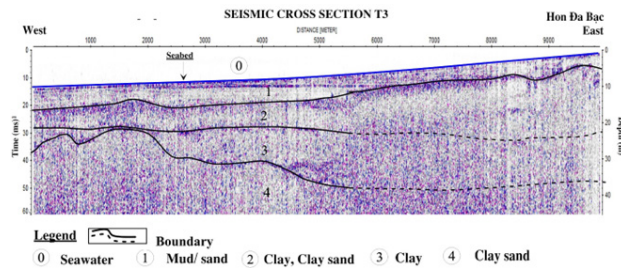


Fig. 7. The structural cross-section for seismic measurement line T3

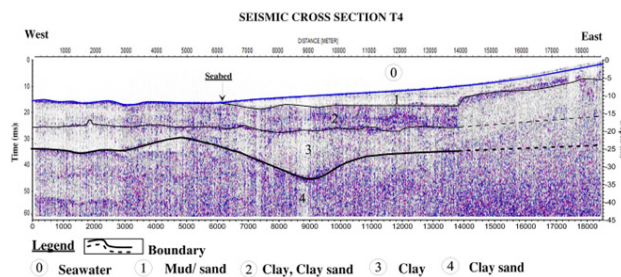


Fig. 8. The structural cross-section for seismic measurement line T4

#### Middle – Upper Pleistocene, Longtoan formation (Q12–3lt)

In Camau province area, the top of the Q12–3lt deposits is located at the depth 42–70 m (average 54 m). Thickness varies between 21–94 m, with an average of 49 m. The Q12–3lt deposits unconformably overlays the sediments of the Camau formation (Q11cm). The formation is divided in two facies: alluvial-marine (amQ12–3lt) and marine (mQ12–3lt). The lower part consists of fine-grained sediments. The upper part is built of clayey silt, silt, silty sand.

#### Upper Pleistocene, Longmy formation (Q13lm)

In Camau province area, the top of Q13lm deposits is located at the depths 12.5–45 m. Thickness ranges from 15 to 41 m. The sediments of the Longmy formation unconformably overlay the Longtoan formation (Q12–3lt) and are overlaid by Holocene (Q21–2). This Longmy formation is divided it in two facies: alluvial-marine deposits (amQ13lm) and marine deposits (mQ13lm): These depos-

its are mainly composed of fine-grained sediments: clay, silty clay, clayey silt, silt, grey light yellow to golden brown silty sand.

#### Holocene (Q2)

##### Lower to middle Holocene (Q21–2)

In Camau province area, the top of the Q21–2 deposits is located at depths from 1.0 to 6.0 m. The thickness varies from 10 to 40 m. The sediments unconformably overlay Longmy formation. The formation consists mainly of blue-grey fine-grained soils and contains humus. The formation is divided into two facies: The first one are the mixed alluvial-marine deposits (amQ21–2) which is distributed only in a few places: 3 to 10 m in depth. The deposits consist of fine sand and green-grey silty sand containing humus. The second one are the marine deposits (mQ21–2): They are distributed throughout the study area at depths 1.0 to 6.0 m, consisting mainly of mud, clay, silty sand and silt.

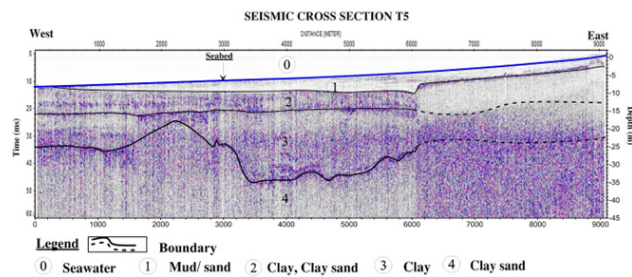


Fig. 9. The structural cross-section for seismic measurement line T5

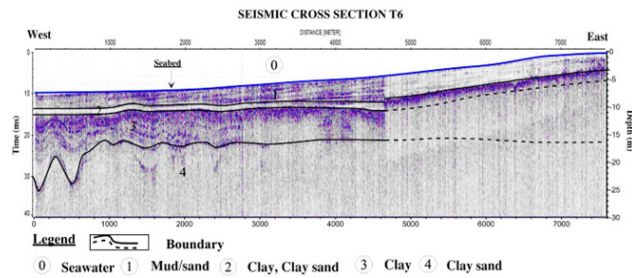


Fig. 10. The structural cross-section for seismic measurement line T6

#### Middle to upper Holocene (Q22–3)

There is only one facies in this sub-epoch. Alluvial-marine deposits (amQ22–3): These deposits are exposed at the surface in almost all areas and are mainly composed of clay and grey-golden fine sand interbedded with thin dark brown clay layers, which contains iron concretions of gravel size. They are easily compressible sediments, flexible, and very plastic. At some places good quality clay is mined. Sediment thickness varies between 1.0 m and 5.0-6.0 m.

#### Upper Holocene (Q23)

There are two facies of these most recent sediments: (1) alluvial-marine-swamp deposits (ambQ23)

distributed mainly in the northeast and the northwest region. The major components of these deposits are clay, silt, brown-grey fine sand, humus, and poorly decomposed plants. Sediment thickness varies between 1.0 and 1.5 m and (2) alluvial deposits (aQ23) which are distributed along the banks of the rivers and canals in the form of narrow strips of alluvial sediments. Sediment composition is mainly silt; clay; little fine sand and humus.

### Results and discussion

The location of the 6 lines along which the Sub-bottom Profiler made the measurements in the study area, in the western shallow waters of Camau, adjacent to Thailand Gulf is presented in Figure 4. The measuring lines are all in the west-east direction and have a definite length (Table 1).

In the Figures 5-10 seismic cross-sections with the primary geological interpretation using ReflectW software of 6 sub-bottom profiler lines are presented.

The structural cross-sections of 6 seismic measurement lines are divided into 5 layers with different thicknesses and compositions (Pinson et al., 2008), and are summarized in Table 1.

In the plots of all six high-resolution shallow seismic profiles, the recorded reflected signal is up to 120 ms in length. But, the well-reflected signals, used in the analysis, are in the range of 20-70 ms, showing quite uniformity in

physical characteristics and petrological nature of the survey environment.

Overall, the seismic wave field in the study area is relatively clear, except from some parts of the measured lines due to the strong absorption of wave energy, when passing through the surface of the seabed, which proves the main sedimentary formation is rough grain sand, sand and gas with poor attachment, that makes the research depth of the method limited. Thus, the seismic wave field in the sections shows the nature of the fine- or coarse-grained petrological composition, when the seismic wave is transmitted. In the survey area, there are wedge-shaped, oblique, corrugated and transverse structures.

The boundaries in the shallow sedimentary sediment structure are important targets to be achieved when using the surveyed measurement data with High-Resolution Shallow Reflection Seismics. Therefore, while interpreting the seismic cross-sections, we have relied on the stratigraphic column of some neighboring boreholes and the geological structure characteristics of the study area as the basis for linking and interpreting the lines as soon as boundaries according to structural layers by seismic data. This is especially useful for measurement lines where the received seismic wave field signal is not clear or is too faint when noise sources are excluded. The combination of information about geological structure and the hole floor and the seismic data has contributed to the accuracy of the boundary positions of the sedimentary structure layers in the shallow water band near the shore and has already been achieved necessary reliability.

Overall, the above analysis shows that the terrain of the seabed in the survey area tends to be shallow from the West to the East (from the sea to the shore) the slope is low, relatively flat, there is no sign of digging and undulating on the surface of the seabed. Except, the two positions at beginning of T1 line show that the head of the route has quite a steep and deep terrain, which may be the slope of the continental shelf in the survey area and at the beginning of the T6 measuring line, there are also two small-scale geological faults with a displacement amplitude in the range of 1.5 to 4 m.

Tab. 1. Characteristics of structural sections according to Sub-bottom profiler data

Seismic line	Layer 0	Layer 1	Layer 2	Layer 3	Layer 4
T1, length 2600m	Seawater, and sea-level depths ranging from 2-14 m.	The thickness ranges from 1.8 to 4 m. The weak reflective boundary shows, that the sediments are mainly coarse particles. The lithology is mainly sand, silt, corresponding to Holocene sediments.	The thickness ranges from 4 to 14 m. The lithology is mainly clay mud, and soft clay, corresponding to the Holocene age sediments.	The thickness ranges from 4 to 10 m. There is a boundary of strongly reflected seismic waves. The lithology is mainly sandy, and clayey, corresponding to the Holocene sediments. The bottom is the boundary between the Holocene and Pleistocene sediments.	Starting from 20 m down, the seismic wave is completely absorbed. The lithology is sandy clay, and sand powder, corresponding to the Pleistocene sediments.
T2, length 12000 m	Seawater and sea-level depths ranging from 2-14 m.	The thickness ranges from 5-8 m, the formation has the form of horizontal layers stacked on top of each other, shown through the strongly reflected seismic wave field. The lithology is mainly clay mud, and soft clay.	The thickness ranges from 1-3 m, the lithology is mainly clay, and soft clay. In the second half of the line the boundary of reflection is completely absorbed, showing that the sediment has poor cohesion and high porosity. The lithology is mainly powdery sand, and mixed sand, corresponding to the Holocene sediments.	The thickness ranges from 2-25 m, the lithology is clay-sand. In this layer, the seismic wave field is also strongly absorbed, making the reflection boundary of the two media weak. The bottom is the boundary between the Holocene and Pleistocene sediments.	Starting from a depth of 20 m down the seismic wave completely lost its signal, the lithology is mainly clay, and solid-phase clay, corresponding to the Pleistocene sediments. There is an intrusive bedrock block in the beginning of the line.
T3, length 10000 m	Seawater, and sea-level depths ranging from 2-14 m.	The thickness ranges from 5-9 m, the formation has the form of horizontal layers stacked on top of each other. The lithology is mainly mud and sand, corresponding to the Holocene sediments. At the end of the line, the bedrock surface was discovered near Hon Da Bac.	The thickness ranges from 8-18 m, the boundary of the reflection is clear, the lithology is mainly sandy clay, and sand, corresponding to the Holocene sediment.	The thickness ranges from 0.5-15 m, the lithology is clay-sand. The seismic wave field is also strongly absorbed, making the reflection boundary of the two media weak. The bottom is the boundary between the Holocene and Pleistocene sediments.	From the depth of 30m down, the seismic wave completely lost its signal, the lithology is mainly clay, and hard clay, corresponding to the Pleistocene sediments.
T4, length 19000 m	Seawater, and sea-level depths ranging from 2-12 m.	The thickness ranges from 0.5-6 m, the formation has a horizontal layered form. The lithology is mainly mud, and fine grain sand-mud.	The thickness ranges from 6-11 m, the reflective boundary is clear, the lithology is mainly clay, and soft clay, corresponding to the Holocene sediments. Also gas is present, because the seismic wave is completely absorbed.	The thickness ranges from 4-20 m, petrology is clay-silt sand, silty sand, corresponding to the Holocene sediments. The bottom is the boundary between the Holocene and Pleistocene sediments.	From the depth of 23m down, the seismic wave completely lost its signal, the lithology is mainly clay, and hard clay, corresponding to the Pleistocene sediments.
T5, length 9200 m	Seawater, and sea-level depths ranging from 2-9 m.	The thickness ranges from 2-5 m, the formation has a horizontal layered form. The lithology is mainly mud, and fine grain sand- mud.	The thickness ranges from 5-10 m, the reflection boundary is clear. The lithology is mainly clay, and soft clay, corresponding to the Holocene sediments. Also gas is present.	The thickness ranges from 4-35 m, lithology is sandy sand, sand powder, corresponding to Holocene sediments. The bottom is the boundary between the sediments of the Holocene and Pleistocene.	From the depth of 25m down, the seismic wave completely lost its signal, the lithology is mainly clay, and hard clay, corresponding to the Pleistocene sediments.
T6, length 7800 m	Seawater, and sea-level depths ranging from 2- 8 m.	Thickness ranges from 3-5 m, the formation has a thin layer form recognized by strongly reflected seismic wave field. The lithology is mainly fine-grained mud, and sand, corresponding to the Holocene sediments.	Thickness ranges from 1.5-2.5 m, the lithology is mainly clay, clay powder, and sandy clay. However, from the 4,600th meter to the end of the line, the seismic wave field is completely absorbed, showing that the sediment is poor, high porosity, gaseous, corresponding to the Holocene age sediments.	Thickness ranges from 8-22 m, the lithology is clay-silt sand, corresponding to the Holocene sediments. The bottom is the boundary between the Holocene and Pleistocene sediments.	From a depth of 15-25 m down, seismic waves completely lost their signal. The lithology is mainly clay, and hard compact clay, corresponding to the Pleistocene sediments.

## Conclusion

High-resolution shallow reflection seismic method by sub-bottom profiler instrument system has been used to study the geological structure and engineering geology in the coastal zone with shallow water level in the western sea of Camau. The data series collected on the 6 west-east lines with a total length of 60.6 km has been processed and interpreted on the basis of wave propagation velocity as well as density of the associated geological environment. The main goal of the study – the geological structure of the sub-bottom formation determination was obtained. The relationship with materials such as silt, mud, clay sand, clay powder, sand powder, and sand with different grain size levels and bedrock surface has been determined quantitatively. Boundary interfaces in sedimentary structures with ages from the Pleistocene to Holocene have been determined on the basis of division of 4 structural layers from the seabed in the survey area. The shallow marine sedi-

ments, the Mekong delta sediments to the tidal flat sediments and the boundary of the ancient Pleistocene alluvial surface are clearly divided on all measured structural sections. The boundary between the Holocene and Pleistocene sediments at an average depth of 25-35 m appear on all measurements lines in the study area.

The topography of the seabed in the survey area is relatively flat, has a low slope and tends to gradually shallower from west to east, from the sea to the mainland. The clay layer has a semi-hard to hard state, corresponding to the ancient alluvial surface, at an average depth of 30 m, creating favorable conditions for the construction of coastal works. However, at the beginning of the T6 measuring line, there are also two small-scale geological faults with a displacement amplitude in the range of 1.5 to 4 m, which may be a kind of obstacle for the constructions.

## Literatura – References

1. 3200-xs sub-bottom system user hardware manual, (2005). EdgeTech, 4 Little Brook Road, West Wareham, MA 02576. [www.edgetech.com](http://www.edgetech.com)
2. Alves D.P.V., Caldato E.B., de Moura D.S., dos Santos R.P.Z., Jovane L., (2020). High-Resolution Sub-Bottom and Magnetometer Data From Southeastern Brazilian Coast. *Frontiers in Marine Science*. 7:536295. doi: 10.3389/fmars.2020.536295.
3. Alves D.P.V., de Mahiques M.M., (2019). Deposition and sea-level evolution models for Upper Pleistocene/Holocene in the São Sebastião Channel (SE Brazilian coast) inferred from 5th order seismic stratigraphy. *J. South Am. Earth Sci.* 93, 382–393. doi: 10.1016/j.jsames.2019. 05.012.
4. Amri U., (2019). Recent Sediment Analysis, Study Case: Sub Bottom Profiler Data Line 8 Geomarine Research Vessels. *Journal of Wetlands Environmental Management*, Vol. 7 (2), 123-133. <http://dx.doi.org/10.20527/jwem.v7.v2.171>.
5. Angulo R.J., Lessa G.C., De Souza M.C., (2006). A critical review of mid- to late-Holocene sea-level fluctuations on the eastern Brazilian coastline. *Quat. Sci. Rev.* 25, 486–506. doi: 10.1016/j.quascirev.2005. 03.008
6. Aquino da Silva A.G., Stattegger, K., Schwarzer, K., Vital, H., (2016). Seismic stratigraphy as indicator of late Pleistocene and Holocene sea level changes on the NE Brazilian continental shelf. *J. South Am. Earth Sci.* 70, 188–197. doi: 10.1016/j.jsames.2016. 05.001
7. Ding W., Zhao D., Wang M., Liu Z., (2021). Chapter 4 Side-scan Sonar and Sub-bottom Profiler Surveying. In Z. Wu et al., *High-resolution Seafloor Survey and Applications*. Science Press 2021, Springer Singapore. [https://doi.org/10.1007/978-981-15-9750-3\\_495](https://doi.org/10.1007/978-981-15-9750-3_495)
8. Dung B.V., Stattegger K., Unverricht D., Phach P.V., Thanh N.T., (2013). Late Pleistocene–Holocene seismic stratigraphy of the Southeast Vietnam Shelf. *Global and Planetary Change* 110 (1), 156-169, DOI: 10.1016/j.gloplacha.2013.09.010.
9. Grelowska G., Kozaczka E., (2010a). Sounding of layered marine bottom – model investigations, *Acta Physica Polonica A*, 118, 66–70.
10. Grelowska G., Kozaczka E., (2014). Underwater acoustic imaging of the sea, *Archives of Acoustics*, 39, 4, 439–452. DOI:10.2478/aoa-2014-0048.
11. Grelowska G., Kozaczka E., Szymczak W., (2010). Method of data extraction from sub-bottom profiler's signal, *Hydroacoustics*, 13, 109-118.
12. Kadima E., Delvaux D., Sebagenzi S.N., Tack L., Kabeya S.M., (2011). Structure and geological history of the Congo Basin: an integrated interpretation of gravity, magnetic and reflection seismic data. *Basin Res.* 23, 499–527. doi: 10.1111/j.1365-2117.2011.0 0500.x
13. Kozaczka E., Grelowska G., Kozaczka S., Szymczak W., (2013). Detection of objects buried in the sea bottom with the use of parametric echosounder, *Archives of Acoustics*, 38, 1, 99–104. DOI: 10.2478/aoa-2013-0012.
14. Lap N.V., Oanh T.T.K., Tateishi M., (2000). Late Holocene depositional environments and coastal evolution of the Mekong River Delta, Southern Vietnam. *J. Asian Earth Sci.* 18, 427–439. doi:10.1016/S1367-9120(99)00076-0.
15. LeBlanc L.R., Mayer L., Rufino M., Schock S.G., King J., (1992). Marine sediment classification using the chirp sonar, *The Journal of the Acoustical Society of America*, 91(1), 107-115.
16. Lurton X., (2002). *An Introduction to Underwater Acoustics: Principles and Applications*. Springer, Praxis, Chichester, UK.
17. Moley C.K., (2002). A Tectonic model for the Tertiary evolution of strike – slip faults and rift basins in SE Asia. *Tectonophysics* 347(4), 189-215. DOI: 10.1016/S0040-1951(02)00061-6
18. Pinson L.J.W., Henstock T.J., Dix J.K., Bull J.M., (2008). Estimating quality factor and mean grain size of sediments from high-resolution marine seismic data. *Geophysics*, vol. 73, no. 4, pp. 19–28.
19. Saleh M., Rabah M., (2016). Seabed sub-bottom sediment classification using parametric sub-bottom profiler. *NRIAG Journal of Astronomy and Geophysics, Egypt* (5) 87-95. <http://dx.doi.org/10.1016/j.nrjag.2016.01.004>.
20. Stattegger K., Tjallingii R., Saito Y., Wetzels A., Michelli M., Thanh N.T., (2013). Mid to late Holocene sea-level reconstruction of Southeast Vietnam using beachrock and beach-ridge deposits. *Global and Planetary Change* 110 (1), 214–222. DOI: 10.1016/j.gloplacha.2013.08.014
21. Wagner F., Vuong B.T., Renaud F.G., (2012). Groundwater Resources in the Mekong Delta: Availability, Utilization and Risks, in: *The Mekong Delta System*, Springer Environmental Science and Engineering. Springer, pp. 201–220.
22. Wang F., Dong L., Ding J., Zhou X., Tao C., Lin X., Liang G., (2019). An Experiment of the Actual Vertical Resolution of the Sub-bottom Profiler in an Anechoic Tank. *Archives of Acoustics*, Vol. 44, No. 1, pp. 185–194, DOI: 10.24425/aoa.2019.126364.



23. Murena, F. (2004). Measuring air quality over large urban areas: Development and application of an air pollution index at the Environ Monit Assess (2018) 190:625 Page 9 of 10 625 urban area of Naples. Atmospheric Environment, 38(36), 6195–6202.
24. Stankevich, S., Titarenko, O., Kharytonov, M., Bensehoub, A., Bounouala, M., Chaabia, R., & Boukeloul, M. L. (2015). Mapping of urban atmospheric pollution in the northern part of Algeria with nitrogen dioxide using satellite and ground-truth data. Studia Universitatis "Vasile Goldis" Arad. Seria Stiintele Vietii (Life Sciences Series), 25(2), 87.
25. Stankevich, S., Titarenko, O., Svideniuk, M., Kharytonov, M., Bensehoub, A., & Khlopova, V. (2016). Air pollution mapping with nitrogen and sulfur dioxides in the south-eastern part of Ukraine using satellite data. Mining Science, 23.
26. Sulejmanović, J., Muhić-Šarac, T., Memić, M., Gambaro, A., & Selović, A. (2014). Trace metal concentrations in size-fractionated urban atmospheric particles of Sarajevo, Bosnia and Herzegovina. International Journal of Environmental Research, 8(3), 711-718.
27. World Health Organization. (2016). Ambient air pollution: a global assessment of exposure and burden of disease. World Health Organization. <https://apps.who.int/iris/handle/10665/250141>.